# NACA

### RESEARCH MEMORANDUM

LATERAL CONTROL CHARACTERISTICS OF TWO

STRUCTURALLY SIMILAR FLEXIBLE WINGS WITH 45° SWEEP:

A SWEPTBACK WING AND A WING WITH M PLAN FORM

By Rodger L. Naeseth, Delwin R. Croom, and John W. McKee

Langley Aeronautical Laboratory
Langley Field, Va.

## NATIONAL ADVISORY COMMITTEE FOR AERONAUTICS

WASHINGTON

April 26, 1954 Declassified November 14, 1956

#### NATIONAL ADVISORY COMMITTEE FOR AERONAUTICS

#### RESEARCH MEMORANDUM

LATERAL CONTROL CHARACTERISTICS OF TWO STRUCTURALLY SIMILAR FLEXIBLE WINGS WITH  $45^{\circ}$  SWEEP:

A SWEPTBACK WING AND A WING WITH M PLAN FORM

By Rodger L. Naeseth, Delwin R. Croom, and John W. McKee

#### SUMMARY

A low-speed wind-tunnel investigation was made to determine the static lateral control characteristics of flap-type and retractable spoiler-type ailerons on a rigid sweptback wing, a flexible sweptback wing, and a flexible M-wing. A few tests were also made with a half-delta tip control on the flexible sweptback wing. The semispan wing models were of aspect ratio 6.0, taper ratio of 0.6, and had NACA 65A009 airfoil sections parallel to the free-stream direction. The quarter-chord lines of the wings were swept 45° and the break in the M-wing was at the half semispan location.

At low angles of attack, flap-type ailerons and retractable spoilertype ailerons lost effectiveness with increase of dynamic pressure on both the flexible sweptback plan-form wing and the M plan-form wing. Spoilers, however, tended to maintain a greater percent of rigid-wing control effectiveness. An inboard location of the controls was better than a location near the tip, and the M-wing was better than the swept wing in maintaining effectiveness.

The theoretical variations of fraction of rigid rolling-moment coefficient retained by the various spans of flap-type ailerons on the swept-back plan-form wing agreed well over the test range with the experimental values; however, higher reversal speeds were indicated by theory.

#### INTRODUCTION

The use of thin swept wings in airplanes and missiles being designed for high-speed flight has led to a need for greater knowledge of the effects of wing flexibility on the wing aerodynamic characteristics. Also, it has been suggested that wings of M or W plan form be investigated

because these plan forms may possess advantages over straight swept wings. Reference 1 presents the results of an investigation to determine the aerodynamic characteristics in pitch of three semispan flexible wings of sweptback and composite (M and W) plan forms and a rigid wing geometrically similar to the flexible sweptback wings.

The present paper presents the results of an investigation to determine the variation with dynamic pressure of the lateral control characteristics of the sweptback wings and the M plan-form wing of reference lequipped with flap-type and spoiler-type ailerons of various spans and spanwise locations. A half-delta tip aileron was also investigated on the flexible sweptback wing.

#### COEFFICIENTS AND SYMBOLS

The forces and moments measured on the wing are presented with respect to the wind axes which, for the conditions of these tests (zero sideslip), correspond to the stability axes. (See fig. 1.) The origin of axes was the 25-percent-chord point of the mean aerodynamic chord projected in the plane of symmetry.

The rolling-moment and yawing-moment coefficients presented represent the aerodynamic moments on a complete wing produced by the deflection of the aileron on only the left semispan of the wing.

. Twice semispan lift

$\mathrm{c}_{\mathrm{L}}$	lift coefficient, qS
Cl	rolling-moment coefficient, L/qSb
$\Delta C_{l}$	increment of rolling-moment coefficient
$C_n$	yawing-moment coefficient, N/qSb
L	rolling moment resulting from control deflection, ft-lb
N	yawing moment resulting from control deflection, ft-lb
q	free-stream dynamic pressure, $\rho V^2/2$ , lb/sq ft
S	twice wing area of semispan model, sq ft
Ъ	twice span of semispan model, ft

 $\bar{c}$  mean aerodynamic chord of wing using theoretical tip,  $\frac{2}{5} \int_{0}^{b/2} c^{2} dy$ , ft

c local wing chord, ft

y lateral distance from plane of symmetry, ft

ba span of aileron, ft

V free-stream velocity, ft/sec

ρ mass density of air, slugs/cu ft

angle of attack of wing root chord, deg

δ<sub>a</sub> aileron deflection angle relative to chord plane of wing, deg; measured in a plane perpendicular to aileron hinge axis and positive when trailing edge is down

E Young's modulus of elasticity, lb/sq in.

G shear modulus of rigidity, lb/sq in.

I moment of inertia in bending, in.4

J torsional stiffness constant, in.4

qb4/EI dimensionless scaling factor (note that units of linear measurement used in q, b, E, and I must be consistent)

$$C_{l}\delta_{a} = \left(\frac{\partial C_{l}}{\partial \delta_{a}}\right)_{\alpha=0}^{0}$$
 measured near  $\delta_{a} = 0^{0}$ 

#### Subscripts:

i inboard end of control

o outboard end of control

r root

F flexible wing

R rigid wing

#### MODELS

Flap-type and retractable spoiler-type ailerons were investigated on three semispan wings: a rigid sweptback wing, a flexible sweptback wing, and a flexible M plan-form wing. Geometric characteristics of the wings and ailerons are given in figures 2 and 3.

The three-foot semispan wings were of aspect ratio 6, taper ratio 0.6, and had NACA 65A009 airfoil sections parallel to the freestream direction. The quarter-chord lines of the wings were swept 45° and the break in the M-wing was at the half-semispan location. The spanwise variation of EI and GJ, EI/GJ ratio, and the torsionalaxis location were chosen to be reasonably representative of the characteristics of conventional construction. The wing bending and torsional strength were concentrated in a single spar along the 0.40c line of the wing with the profile of the wing formed by a series of balsa segments attached in such a manner that they did not alter the structural characteristics of the spars. (See fig. 3.) The slots between segments were filled with grease. The variation of EI and GJ with span for the wings is given in figure 4. A complete description of the wing design is given in reference 1. A rigid sweptback wing of the same geometry as the flexible sweptback wing was constructed of mahogany reinforced with steel.

Plain 0.25c sealed ailerons and 0.10c projection retractable spoiler-type ailerons (referred to as spoilers hereinafter) of the various spans and spanwise locations listed in table I were tested on the three wings. The method of hinging the segments which were deflected to make up the various aileron spans is shown in figure 3. This method was used to keep the added weight to a minimum; however, some reduction in the flutter speed resulted. The spoilers were of 1/32-inch aluminum and were broken between each wing segment with sufficient clearance provided so that there was no change in wing stiffness. A half-delta tip aileron (fig. 2) was tested only on the flexible sweptback wing. The half-delta tip control was attached to the spar of the wing by an angle fitting so that the hinge line was normal to the plane of symmetry. The span and area used in computing the coefficients of the half-delta tip aileron included the span and area of the half-delta tip control.

Throughout the present paper the models are referred to as the  $\Lambda\text{-}$  and M-wings and the subscripts R and F are used to differentiate between the rigid and flexible wings.

#### APPARATUS

The investigation was made in the Langley 300 MPH 7- by 10-foot tunnel. In order to test the semispan models in a region outside the tunnel boundary layer, a reflection plane was mounted about 3 inches from the tunnel side wall as shown in figure 5. The reflection-plane boundary-layer thickness was such that a value of 95 percent of the free-stream dynamic pressure was reached at a distance of 1.7 inches from the surface at the balance center line for all test dynamic pressures. This thickness represents a distance of 4.7-percent semispan for the models tested. A 1/8-inch-thick metal end plate was attached to the root of the model to cover the slot cut in the reflection plane for the wing butt (fig. 5). Data were obtained by using a strain-gage balance mounted outside the tunnel wall.

#### TESTS

Tests were performed at dynamic pressures from 4.7 to 30 lb/sq ft. Dynamic pressure for the  $\Lambda_R\text{-wing}$  tests was 11.7 lb/sq ft. Reynolds numbers based on the mean aerodynamic chord of the models varied from 0.4  $\times$  10 $^6$  to 1.02  $\times$  10 $^6$ . Angles of attack and dynamic pressures were limited by the maximum lift of 24 pounds and the flutter speed of the flexible wings.

Lateral-control tests were performed through an angle-of-attack range at constant  $10^{\circ}$  and  $20^{\circ}$  aileron deflections, -0.10c spoiler projection, and -8° and -27.7° half-delta tip-aileron deflection.

#### CORRECTIONS

Jet-boundary corrections, determined by the method of reference 2, have been applied to the angle of attack. Blockage corrections were found to be negligible. No corrections were applied to account for the effects of the end plate attached to the root of the model. The same reflection-plane corrections to rolling moment (table I) were applied to both the aileron and spoiler data; however, no correction was applied to the half-delta tip-aileron data.

#### RESULTS AND DISCUSSION

#### Swept Wings

The variations of rolling- and yawing-moment coefficients with angle of attack are presented in figure 6 for the various spans of ailerons, and in figure 7 for the various spans of spoilers on the  $\Lambda_R$ -wing. Corresponding plots for the  $\Lambda_F$ -wing are given in figures 8 and 9, respectively. Figure 10 is a cross plot at  $\alpha=0^{\circ}$  showing  $C_{l}$  against  $\delta_{a}$  for  $\Lambda$ -wing ailerons.

Rigid-wing characteristics.— The  $\Lambda_R$ -wing was tested primarily to give a rigid (q = 0) point for the flexible-wing tests; however, because there is not a great amount of lateral-control data available for wings of this plan form, a brief discussion of the  $\Lambda_R$ -wing results is included.

The results of figure 6 indicate a reduction in aileron effectiveness,  $C_l/\delta_a$ , with angle of attack for all spans of ailerons. An examination of the data of figures 6 and 10 indicates a reduction of aileron effectiveness as  $\delta_a$  is increased from  $10^{\circ}$  to  $20^{\circ}$ ,  $\alpha = 0^{\circ}$ . Decreasing the span of the outboard ailerons from 0.80b/2 to 0.39b/2 almost halved the aileron effectiveness. Moving this control inboard resulted in somewhat better effectiveness with an intermediate position the most effective.

No rigid-wing tests were made for the half-delta tip aileron; however, a rigid value of  $c_{l\delta_a}$  of 0.0013 was obtained by extrapolating the flexible-wing results of figure 8(e) to q = 0.

The results of figure 7 indicate that spoiler effectiveness increased with increase in span of outboard control. A spoiler of about 0.4b/2 span was considerably more effective when moved inboard,  $y_0 = 0.61b/2$  or  $y_0 = 0.82b/2$ . The 0.82b/2 location of the outboard end of the spoiler was somewhat better for angles of attack up to  $4^{\circ}$ . All spoilers showed rapidly decreasing effectiveness above  $4^{\circ}$  angle of attack that was more pronounced than the loss of effectiveness of the plain ailerons. This loss is typical of unvented spoilers on swept wings and can be alleviated by using a slot through the wing behind the spoiler (ref. 3). As is characteristic of plain spoilers, favorable yawing-moment coefficients were shown over most of the angle-of-attack range.

Aileron effectiveness computed by the methods of references 4 and 5 agreed well with experimental values as shown in table IT.

Effect of wing flexibility. The flexible-wing data were limited in angle of attack for the higher dynamic pressures; however, it is shown that the reduction in  $\mathrm{C}_l$  with angle of attack for the plain ailerons is generally not as great for the  $\Lambda_F$ -wing (fig. 8) as for the  $\Lambda_R$ -wing (fig. 6) and the values were nearly constant over a greater range of angle of attack as q was increased. Effectiveness was maintained to higher root angles of attack because wing twist reduced the effective angle of attack of the wing.

The  $C_l$  against  $\delta_a$  curves, figure 10, indicate that, although flexibility reduces aileron effectiveness, flexible-wing ailerons generally maintain their effectiveness to higher values of  $\delta_a$  than do rigid-wing ailerons. The principal effect of wing flexibility on the spoiler aileron, figure 9, was to delay the loss in effectiveness with angle of attack to about  $8^\circ$ . Even so, the flap-type ailerons maintained a more nearly constant rolling moment over a greater range of angle of attack in that they did not show a loss at low negative angle of attack and had a less abrupt loss at high positive angle of attack.

As an aid in assessing the degree of flexibility present in a wing and the magnitude of aeroelastic effects, it is helpful to examine the variation of aerodynamic characteristics with a nondimensional ratio that includes the major factors influencing deformation of the wing shape. Similar flexible wings (where similarity includes the EI/GJ ratio) will have similar spanwise deflection curves if the dimensionless scaling factors  $qb^{1/2}$ EI are equal. The test results are plotted against this scaling factor using the root value of EI; however, if a comparison is to be made with another wing having a somewhat different variation of EI along the span, using the root value of EI to determine the scaling factor may be misleading and some other spanwise station might be chosen for closer average agreement of  $qb^{1/2}$ EI over the wing span.

The results of figure 11 indicate that all controls lose effectiveness with increasing scaling factor. Because  $\rm b^4/(EI)_r$  is a constant for a given wing, the variations of  $\rm C_l$  and  $\rm C_{l_F}/\rm C_{l_R}$  with  $\rm qb^4/(EI)_r$  are similar to plots of these values against q. Of the 0.4b/2 span controls, the most inboard location was least affected by q, and an aileron deflection of 20° and a spoiler projection of -0.10c yielded almost identical results. Although this inboard location was not the best for  $\rm qb^4/(EI)_r=0$ , it did produce the greatest rolling-moment coefficient of the 0.4b/2 span controls at the higher values of scaling factor.

Reversal was indicated for the outboard 0.4b/2 aileron at qb  $^4\!/(\text{EI})_r\approx$  52 to 56, whereas the spoiler results for this control

location indicated a much higher reversal speed. Over the range investigated, the 0.2b/2 to 1.00b/2 ailerons and spoilers maintained the largest  $C_l$ . The half-delta tip control had a large loss in  $C_l$  over the low range of  $qb^{l}/(EI)_r$  but maintained a small value over the remainder of the test range.

#### Effect of Plan Form

The variations of rolling- and yawing-moment coefficients with angle of attack are presented in figures 12 and 13 for the  $M_F$ -wing ailerons and spoilers, respectively. The rolling-moment coefficients for  $\alpha\approx 0^{\rm O}$  are plotted against  $\,\delta_a\,$  in figure 14 for the ailerons.

Rigid-wing characteristics.- Rigid-wing values for the M-wing were obtained by extrapolating to zero q. The extrapolated values are given in table II. A comparison with the  $\Lambda_R$ -wing for the 0.20b/2 to 1.00b/2 ailerons and spoilers indicates a somewhat greater effectiveness for the M-wing.

Flexible-wing characteristics.— The q=4.7 aileron data of figures 8 and 12 show a relatively abrupt loss in  $C_l$  at an angle of attack of about  $12^\circ$  for the M<sub>F</sub>-wing as compared with the more gradual variation with angle of attack for the  $\Lambda_F$ -wing. At  $\delta_a=20^\circ$ , some erratic results were obtained at  $\alpha=4^\circ$  for controls including the outboard 0.25b/2 of the wing. (See figs. 12(a) and (b).) For  $\alpha=0^\circ$ , the plot of  $C_l$  against  $\delta_a$  (fig. 14) indicates a generally linear variation.

Spoiler ailerons on the  $\Lambda_F\text{-wing}$  and on the  $M_F\text{-wing}$  (figs. 9 and 13) showed a generally similar variation of  $C_l$  with angle of attack. However, some effectiveness remained at an angle of attack of 20° (q = 4.7) for the  $M_F\text{-wing}$ ; whereas for the  $\Lambda_F\text{-wing}$ , effectiveness was essentially zero at an angle of attack of  $16^{\circ}$ .

The spoilers and ailerons on the M<sub>F</sub>-wing had similar losses of rolling moment with angle of attack in the high positive range and the spoilers showed a much greater loss in  $C_l$  in the negative range of angle of attack. The variation of  $C_l$  with scaling factor  $qb^4/(EI)_r$  for the M<sub>F</sub>-wing (fig. 15) indicates that inboard controls were little affected by an increase in q; however, the outboard controls showed a considerable loss in  $C_l$  with q. A 0.20b/2 to 1.00b/2 aileron deflected 20° is shown to be nearly equivalent to a spoiler projected -0.10c with the aileron showing a greater tendency to lose effectiveness with increase of dynamic pressure.

Effect of Control and Plan Form on Variation

of 
$$C_{l_F}/C_{l_R}$$
 With  $qb^{l_f}/(EI)_r$ 

The variation of  $C_{l_F}/C_{l_R}$  with scaling factor is given in figure 16 for combinations tested at  $\alpha=0^{\circ}$ . The  $\Lambda_F$ -wing spoiler controls (fig. 16(a)) exhibited a somewhat different behavior than the ailerons with scaling factor, but generally lost effectiveness at about the same rate as the ailerons, except that the use of spoilers was indicated to be advantageous for outboard-control locations. The spoilers showed a trend to higher reversal speeds than did the ailerons.

The M<sub>F</sub>-wing spoilers (fig. 16(b)) showed considerably less loss in rigid rolling-moment coefficient with scaling factor for the 0.20b/2 to 0.75b/2 and 0.20b/2 to 1.00b/2 locations, but showed about the same large loss as the aileron for the 0.50b/2 to 1.00b/2 location and were about the same as the ailerons for the 0.20b/2 to 0.50b/2 location where both types of controls showed a small loss.

Over the MF-wing test range, all controls on the MF-wing showed less loss of C $_{l_{\rm F}}/$ C $_{l_{\rm R}}$  than was shown by controls on the AF-wing.

Theoretical values of  $C_{l_F}/C_{l_R}$  computed for the swept-wing aileron by the methods of references 6 and 7 are presented in figure 16(a). Agreement of theory and experiment was reasonably good over the test range; however, higher reversal speeds were indicated by the theory. Values of aileron effectiveness parameters  $\alpha_{\delta}$  (wing-section angle of attack equivalent to unit aileron deflection) of 0.53 and  $c_{m_{\delta}}$  (wing-section pitching moment caused by unit aileron deflection) of -0.38 were used in computing  $C_{l_F}/C_{l_R}$  by the method of reference 6.

#### CONCLUSIONS

On the basis of results of tests in the Langley 300 MPH 7- by 10-foot tunnel of three wings (a rigid sweptback wing, a flexible sweptback wing, and a flexible M-wing), numerous comparisons are possible of the effect of the following variables or combinations thereof on the effectiveness of ailerons: wing plan form, wing flexibility, type of control, span and spanwise location of control, and angle of attack. Some of the effects noted are presented as follows:

- l. Flap-type ailerons maintained effectiveness better than unvented spoilers on the swept rigid wing through the angle-of-attack range. Wing flexibility helped to reduce the variation through the angle-of-attack range.
- 2. On the swept flexible wing, spoilers and ailerons lost effectiveness with increase of dynamic pressure, with inboard controls least affected. In an outboard location, spoilers maintained effectiveness better than ailerons did. A half-delta tip control lost effectiveness rapidly.
- 3. The controls were less sensitive to dynamic pressure on the M-wing than on the swept flexible wing.
- 4. Spoilers were more effective than ailerons on the M-wing at high angles of attack.
- 5. The theoretical variations of fraction of rigid rolling-moment coefficient retained by the various spans of flap-type ailerons on the sweptback plan-form wing agreed well over the test range with the experimental values; however, higher reversal speeds were indicated by theory.

Langley Aeronautical Laboratory,
National Advisory Committee for Aeronautics,
Langley Field, Va., March 1, 1954.

#### REFERENCES

- 1. McKee, John W., Croom, Delwin R., and Naeseth, Rodger L.: Aerodynamic Characteristics in Pitch of Three Structurally Similar Flexible Wings With 45° Sweep: A Sweptback Wing, a Wing With M Plan Form, and a Wing With W Plan Form. NACA RM L53J02a, 1953.
- 2. Polhamus, Edward C.: Jet-Boundary-Induced-Upwash Velocities for Swept Reflection-Plane Models Mounted Vertically in 7- by 10-Foot, Closed, Rectangular Wind Tunnels. NACA TN 1752, 1948.
- 3. Lowry, John G.: Data on Spoiler-Type Ailerons. NACA RM L53I24a, 1953.
- 4. Lowry, John G., and Schneiter, Leslie E.: Estimation of Effectiveness of Flap-Type Controls on Sweptback Wings. NACA TN 1674, 1948.
- 5. DeYoung, John: Theoretical Antisymmetric Span Loading for Wings of Arbitrary Plan Form at Subsonic Speeds. NACA Rep. 1056, 1951. (Supersedes NACA TN 2140.)
- 6. Groth, Eric: Determination of the Rolling Effectiveness and Aileron Reversal Speed of an Elastic Swept Wing. Memo. Rep. No. MCREXA5-4595-8-10, Air Materiel Command, Eng. Div., U. S. Air Force, Oct. 7, 1949.
- 7. Foss, Kenneth A., and Diederich, Franklin W.: Charts and Approximate Formulas for the Estimation of Aeroelastic Effects on the Lateral Control of Swept and Unswept Wings. NACA TN 2747, 1952.

TABLE I.- REFLECTION-PLANE CORRECTIONS

	у <sub>і</sub> b/2	У <sub>0</sub> b/2	Correction factor (*)	
$\Lambda_{ m R}$ and $\Lambda_{ m F}$ ailerons	0.20 .61 .20 .40	1.00 1.00 .61 .81	0.88 •95 •78 •89	
$\Lambda_{ m R}$ and $\Lambda_{ m F}$ spoilers	0.21 .61 .21 .41	1.00 1.00 .61 .82	0.88 •95 •78 •90	
M ailerons	0.20 .50 .20	1.00 1.00 .75 .50	0.88 .94 .83 .71	
M spoilers	0.19 .50 .19	1.00 1.00 .76 .50	0.88 •94 .83 •71	

 $<sup>^*</sup>C_l = C_{l_{measured}} \times correction factor$ 

TABLE II.- RIGID-WING VALUES OF ROLLING-MOMENT COEFFICIENT

		y <sub>0</sub> b/2	Span, b/2	△C <sub>l</sub>		
	<u>yi</u> b/2			Experiment	Theory	
					Reference 4	Reference 5
$ \Lambda_{R} \text{ ailerons,} $ $ \delta_{a} = 10^{\circ} $			.39	0.0200 .0099 .0107 .0122	0.0207 .0106 .0101 .0116	0.0204 .0101 .0103 .0124
$\Lambda_{ m R}$ spoilers, -0.10c projection			0.79 .39 .40 .41	0.0327 .0119 .0176 .0194		
M ailerons, $\delta_a = 10^{\circ}$		1.00 1.00 .75	0.80 .50 .55 .30	0.0210 .0151 .0160 .0060		
M spoilers,		1.00 1.00 .76 .50	0.81 .50 .57 .31	0.0385 .0186 .0318 .0070		

Note: Values for M wing were obtained by extrapolating to q = 0.

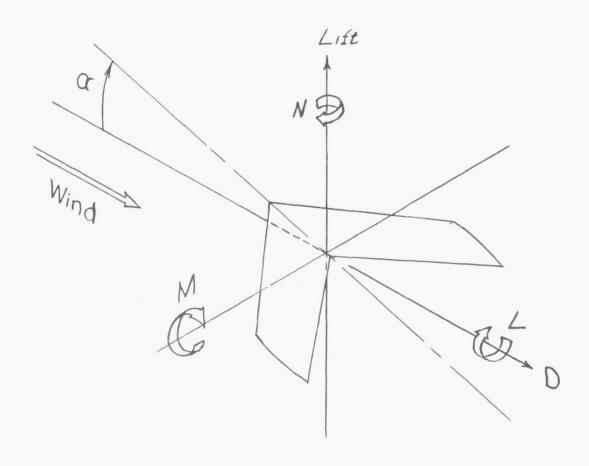
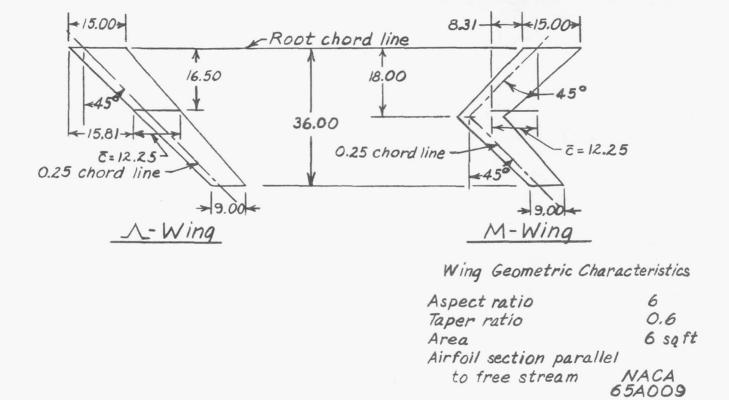
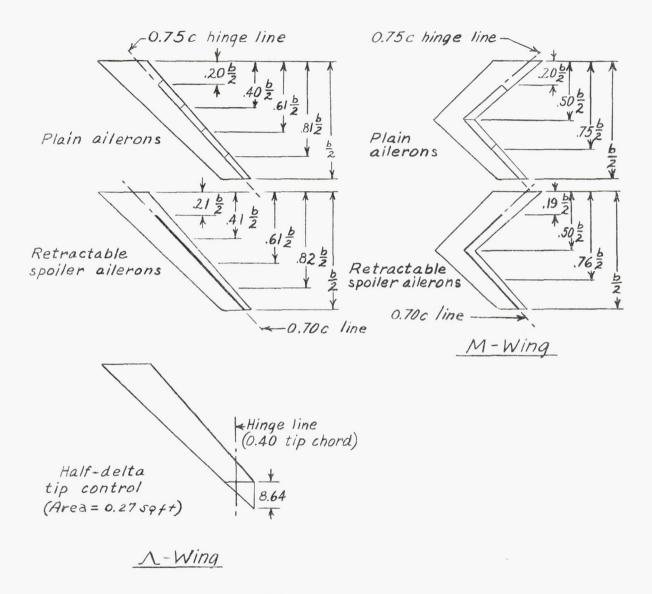


Figure 1.- System of wind axes. Positive values of forces, moments, and angles are indicated by arrows.



(a) Wing details.

Figure 2.- Geometric characteristics of wings and controls.



(b) Control locations.

Figure 2.- Concluded.

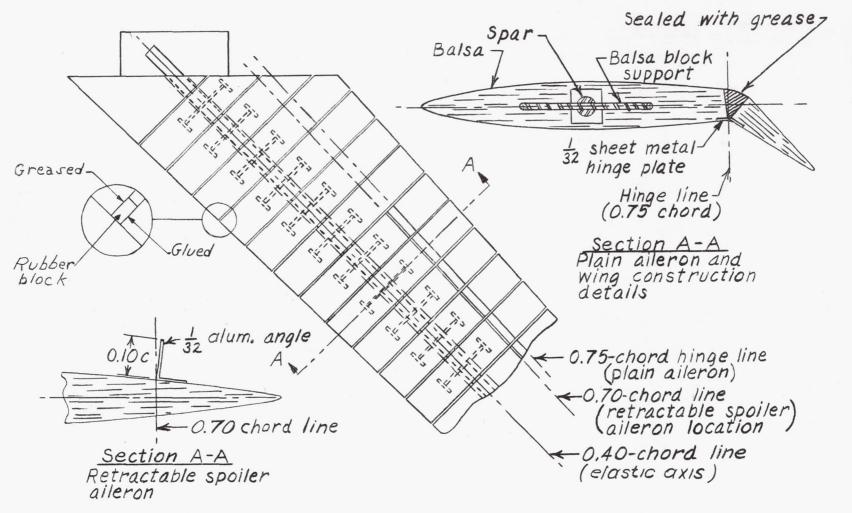


Figure 3.- Wing and control construction details.

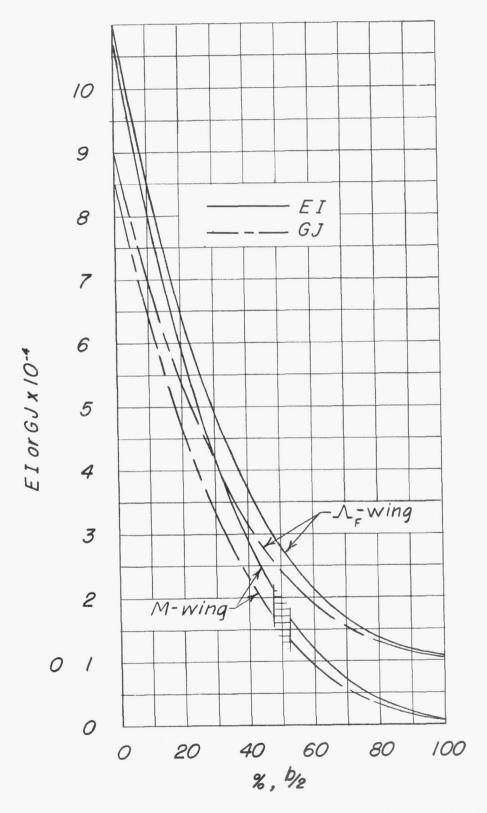
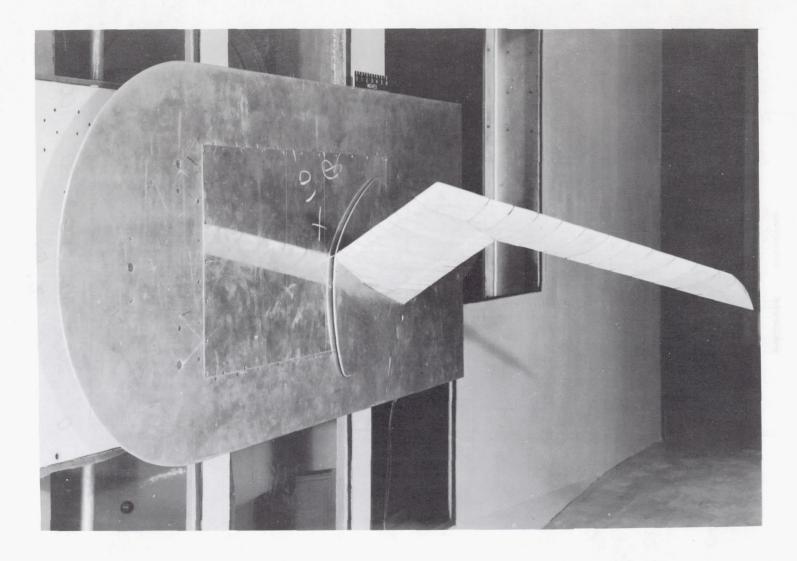


Figure 4.- Spanwise variation of bending and torsional rigidity for  $\Lambda_{\overline{F}^+}$  and M-wings. Values for sections normal to axis of spar.



L-68735
Figure 5.- M-wing test setup in Langley 300 MPH 7- by 10-foot tunnel.

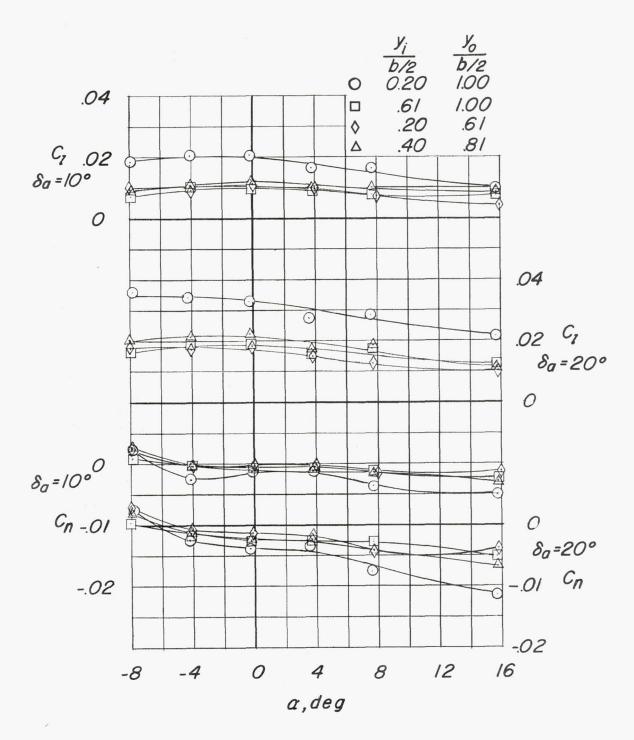


Figure 6.- Variation of lateral control characteristics of  $\Lambda_R$ -wing with angle of attack for various spans of ailerons.

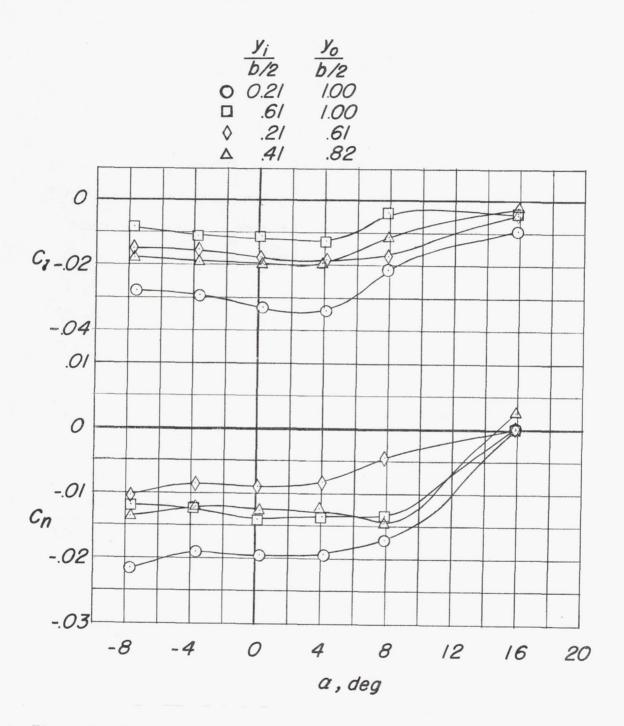
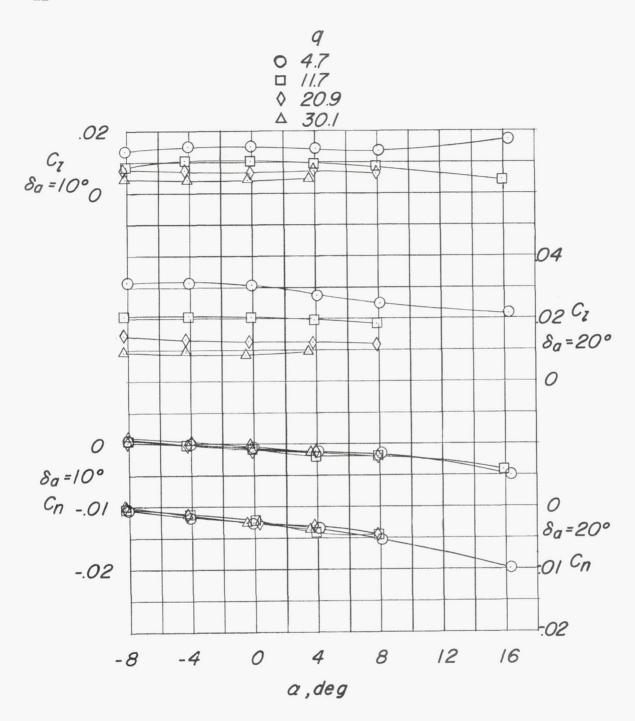
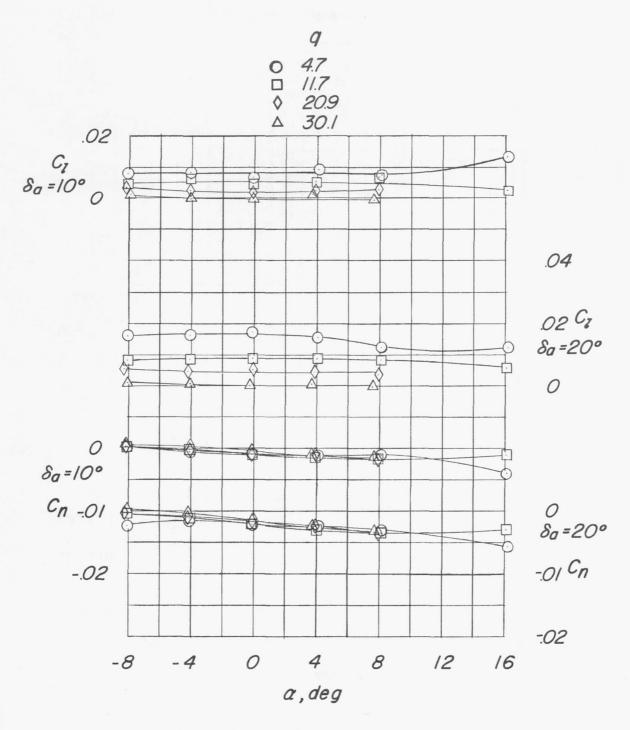


Figure 7.- Variation of lateral control characteristics of  $\Lambda_{\!R}\text{-wing}$  with angle of attack for various spans of spoilers.



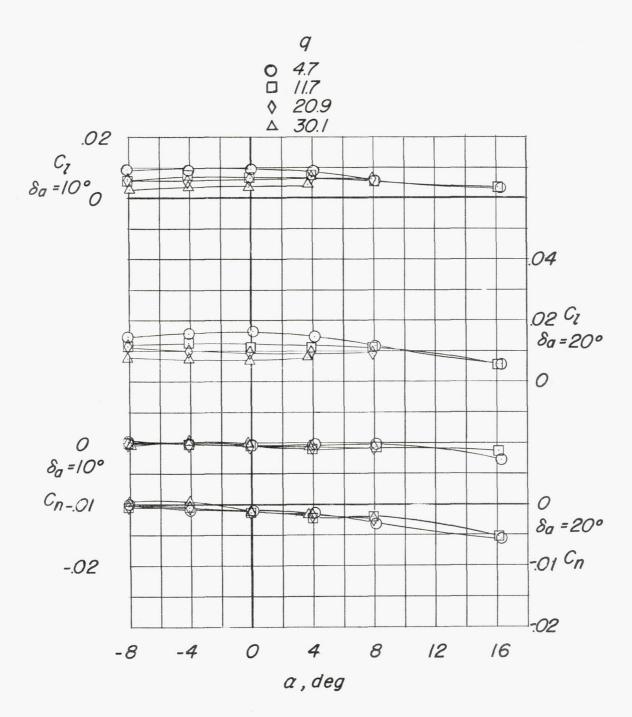
(a) 
$$\frac{y_i}{b/2} = 0.20; \frac{y_0}{b/2} = 1.00.$$

Figure 8.- Effect of dynamic pressure on variation of lateral control characteristics of  $\Lambda_{\rm F}$ -wing with angle of attack for various spans of ailerons.



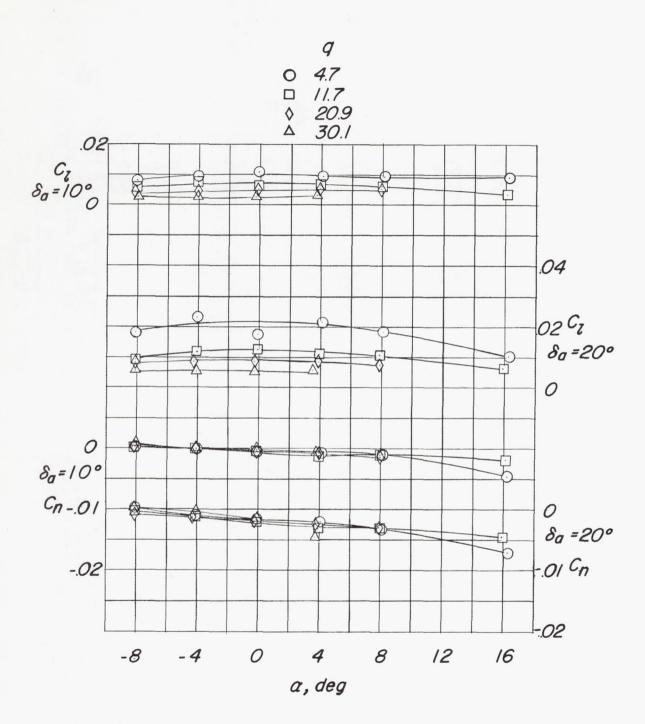
(b) 
$$\frac{y_i}{b/2} = 0.61; \frac{y_0}{b/2} = 1.00.$$

Figure 8.- Continued.



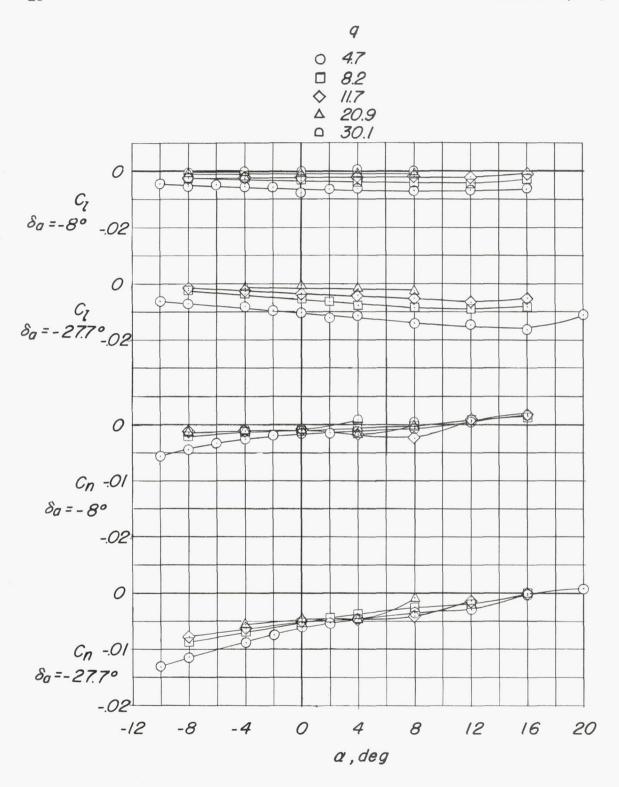
(c)  $\frac{y_i}{b/2} = 0.21; \frac{y_0}{b/2} = 0.61.$ 

Figure 8.- Continued.



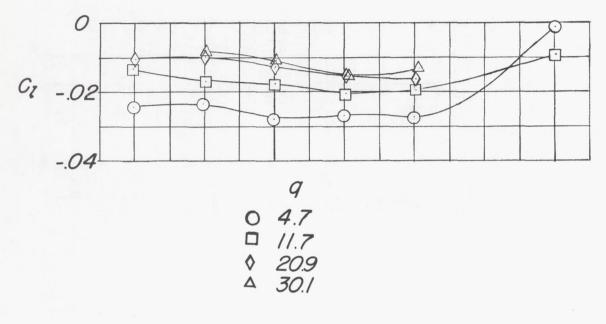
(d) 
$$\frac{y_i}{b/2} = 0.40; \frac{y_0}{b/2} = 0.80.$$

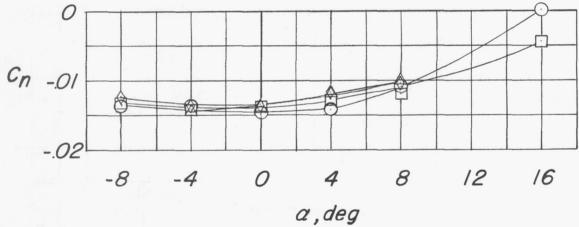
Figure 8.- Continued.



(e) Half-delta tip control.

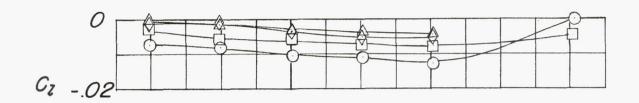
Figure 8.- Concluded.



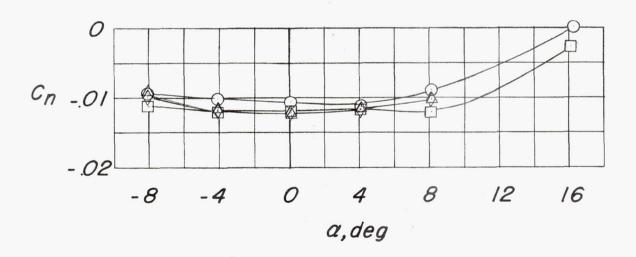


(a) 
$$\frac{y_i}{b/2} = 0.21; \frac{y_0}{b/2} = 1.00.$$

Figure 9.- Effect of dynamic pressure on variation of lateral control characteristics of  $\Lambda_{\overline{F}}$ -wing with angle of attack for various spans of spoilers.

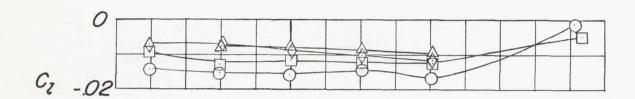


q ○ 4.7 □ //.7 ◊ 20.9 △ 30./

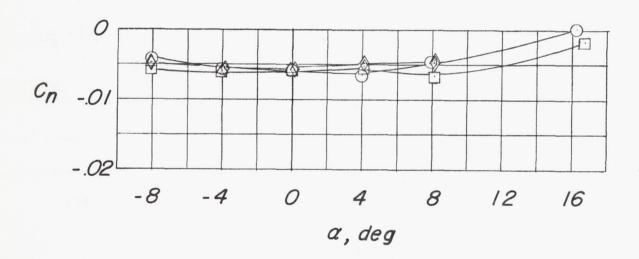


(b) 
$$\frac{y_i}{b/2} = 0.61; \frac{y_0}{b/2} = 1.00.$$

Figure 9.- Continued.

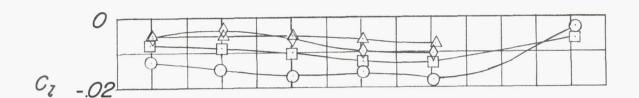


9 0 4.7 □ //.7 ◊ 20.9 △ 30./

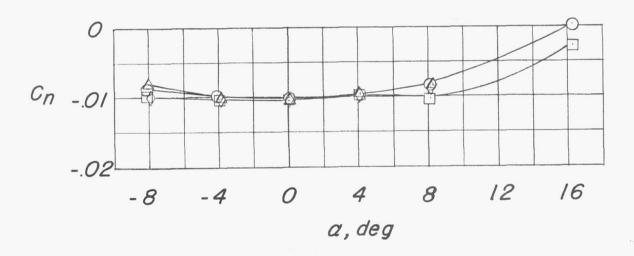


(c) 
$$\frac{y_i}{b/2} = 0.21; \frac{y_0}{b/2} = 0.61.$$

Figure 9.- Continued.



9 0 4.7 □ //.7 ◊ 20.9 △ 30./



(d) 
$$\frac{y_i}{b/2} = 0.41; \frac{y_0}{b/2} = 0.82.$$

Figure 9.- Concluded.

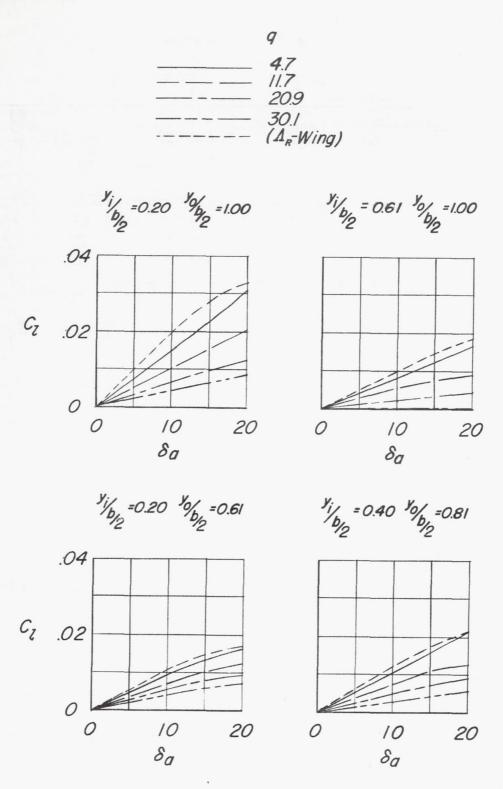


Figure 10.- Effects of dynamic pressure on variation of rolling-moment coefficient with aileron deflection for various spans of ailerons on  $\Lambda$ -wing at  $\alpha$  = 0°.

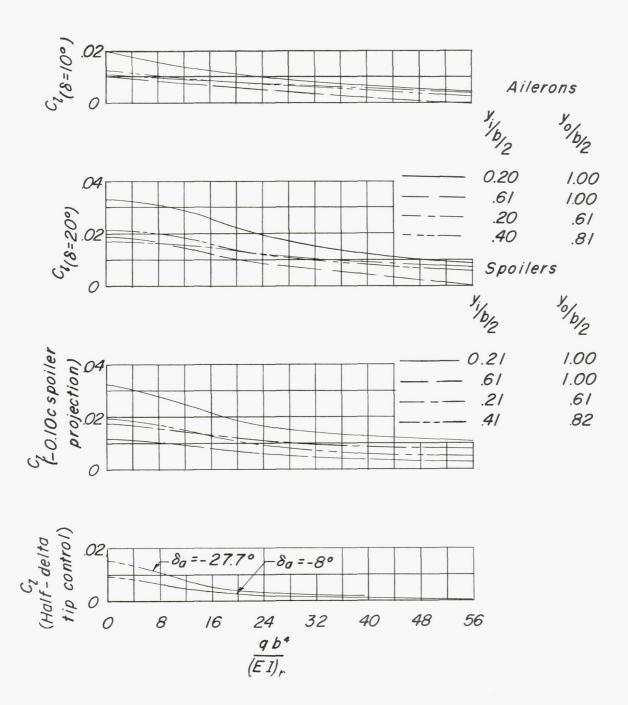
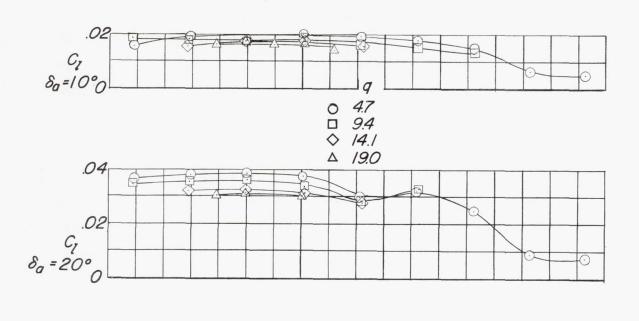
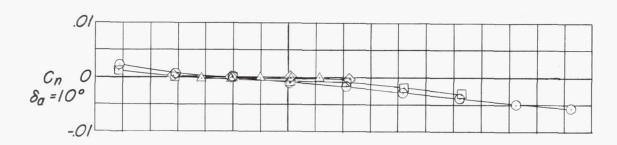
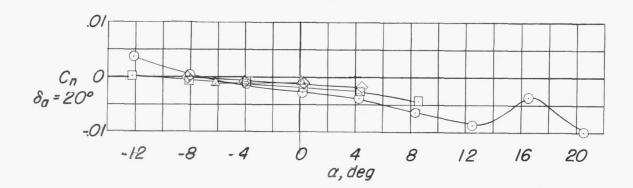


Figure 11.- Variation of rolling-moment coefficient with scaling factor for ailerons and spoilers on  $\Lambda_F\text{-wing}$  at  $\alpha$  = 0°.

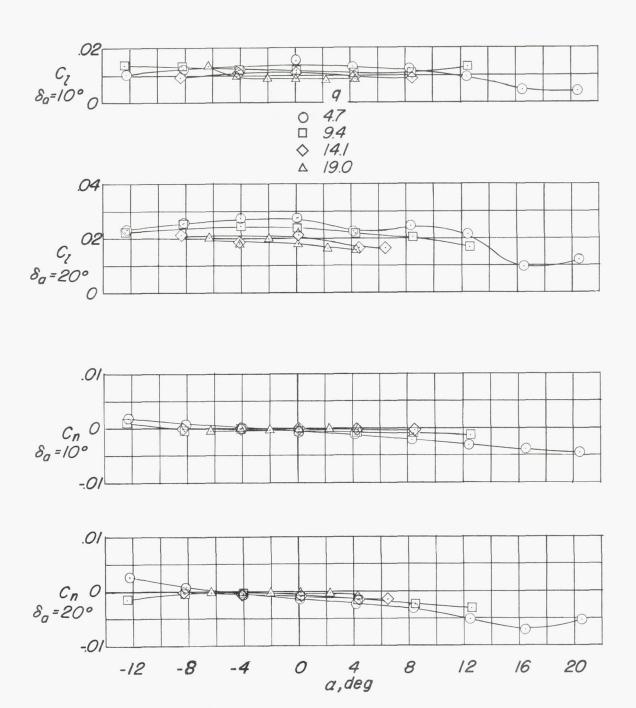






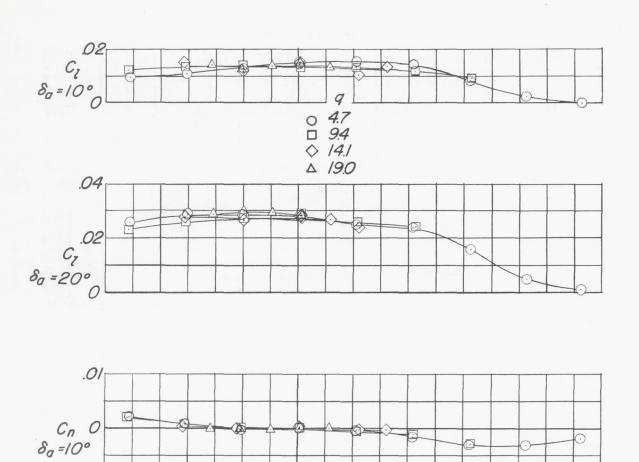
(a) 
$$\frac{y_i}{b/2} = 0.20; \frac{y_0}{b/2} = 1.00.$$

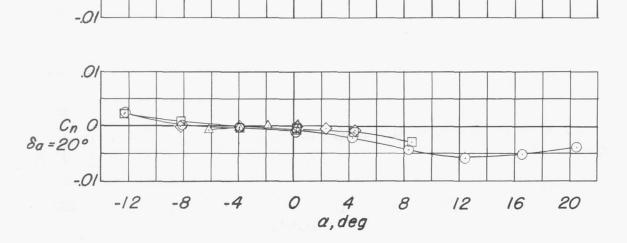
Figure 12.- Effect of dynamic pressure on variation of lateral control characteristics of  $M_{\overline{P}}$ -wing with angle of attack for various spans of ailerons.



(b) 
$$\frac{y_i}{b/2} = 0.50; \frac{y_0}{b/2} = 1.00.$$

Figure 12.- Continued.





(c) 
$$\frac{y_1}{b/2} = 0.20; \frac{y_0}{b/2} = 0.75.$$

Figure 12.- Continued.

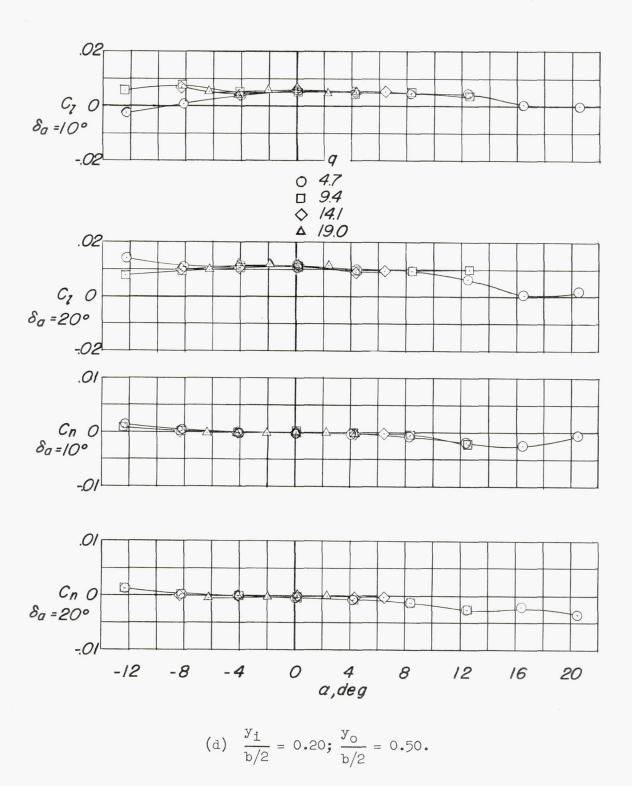
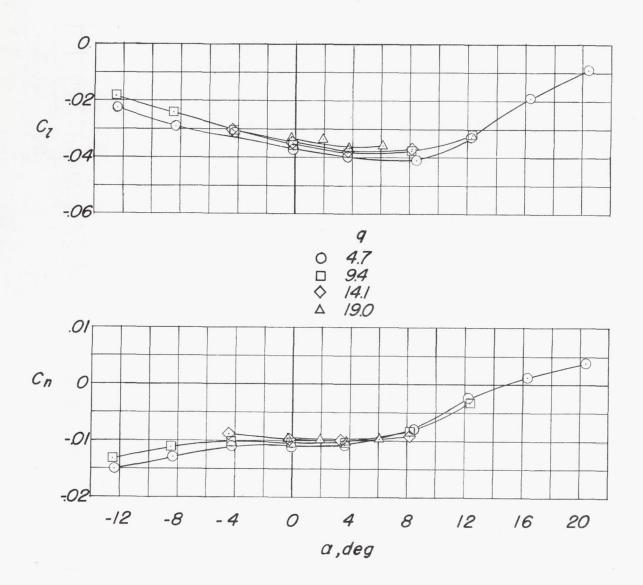
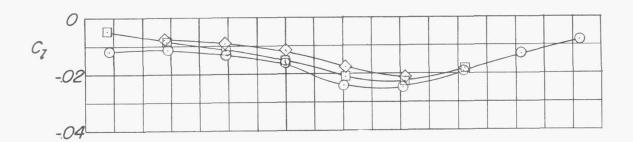


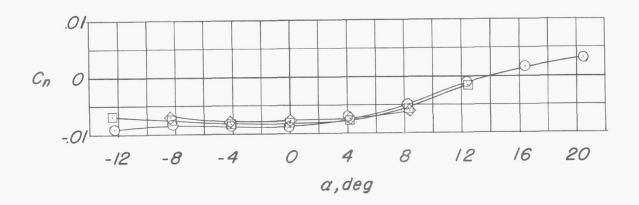
Figure 12.- Concluded.



(a) 
$$\frac{y_i}{b/2} = 0.19; \frac{y_0}{b/2} = 1.00.$$

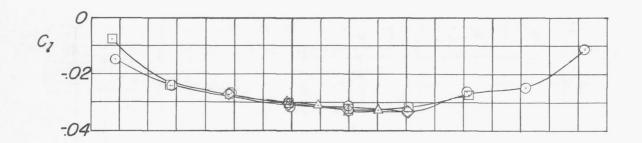
Figure 13.- Effects of dynamic pressure on variation of lateral control characteristics of  $\rm M_{\overline{b}}$  -wing with angle of attack for various spans of spoilers.



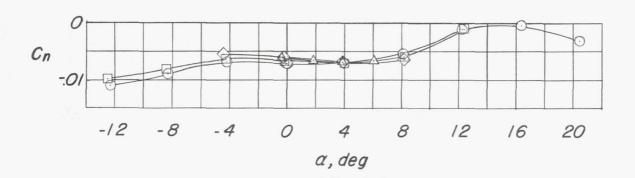


(b) 
$$\frac{y_i}{b/2} = 0.50; \frac{y_0}{b/2} = 1.00.$$

Figure 13.- Continued.

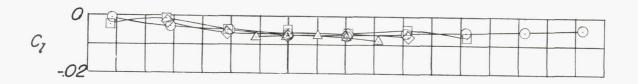


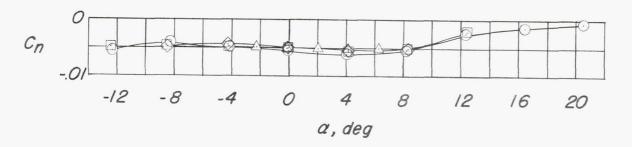
9.4 0 4.7 □ 9.4 0 14.1 △ 19.0



(c) 
$$\frac{y_i}{b/2} = 0.19; \frac{y_0}{b/2} = 0.76.$$

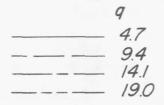
Figure 13.- Continued.





(d) 
$$\frac{y_i}{b/2} = 0.19; \frac{y_0}{b/2} = 0.50.$$

Figure 13.- Concluded.



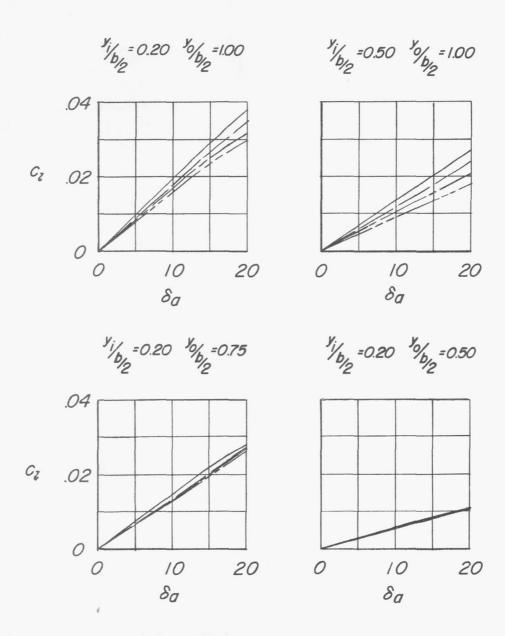


Figure 14.- Effects of dynamic pressure on variation of rolling-moment coefficient with aileron deflection for various spans of ailerons on the  $M_F$ -wing at  $\alpha$  = 0°.

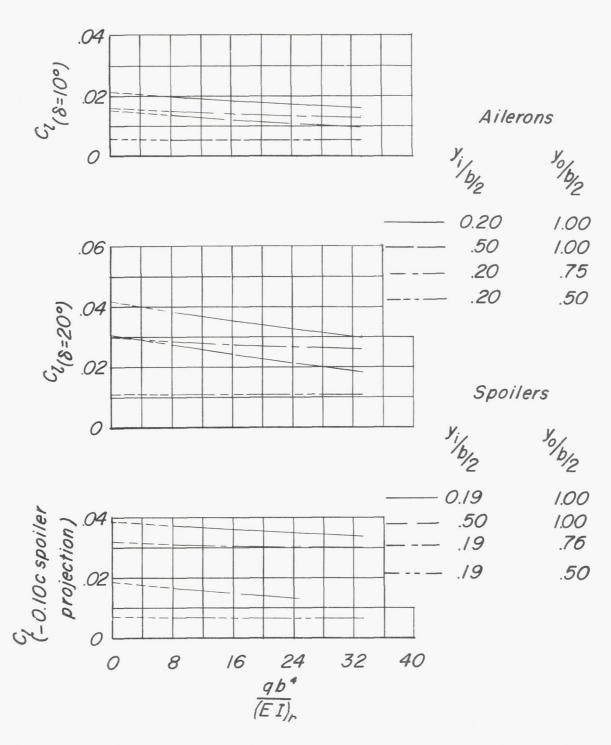
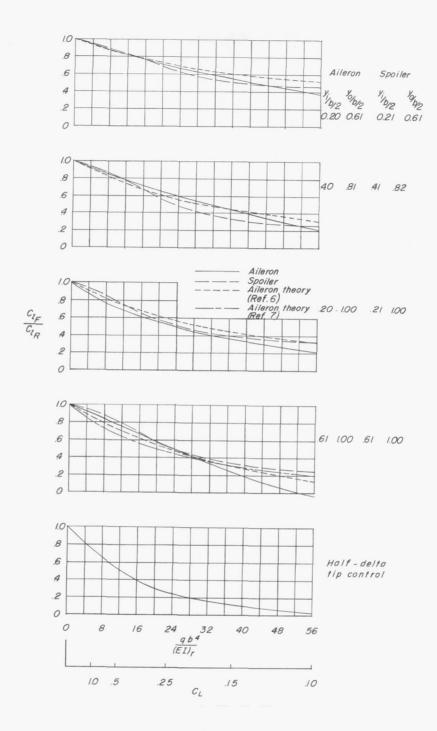
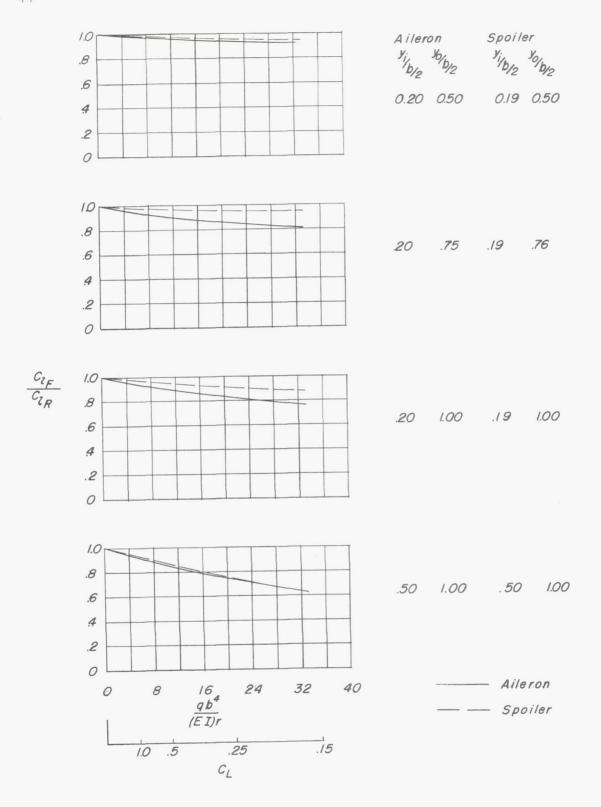


Figure 15.- Variation of rolling-moment coefficient with scaling factor for ailerons and spoilers on  $M_{\overline{F}}\text{-wing at }\alpha=0^{\text{O}}$  .



(a) The 45° sweptback wing.

Figure 16.- Variation of ratio  $C_{l_F}/C_{l_R}$  with scaling factor for ailerons and spoilers on  $\Lambda$ - and M-wings.  $C_L$  is given for level flight; bending stress is 15,000 lb/sq in.;  $\delta_a = -8^\circ$  for half-delta tip control;  $\delta_a = 10^\circ$  for ailerons; -0.10c projection of spoilers.



(b) M plan-form wing.

Figure 16.- Concluded.